Magnetic-field dependence of the critical current in long Josephson junctions

S. Pagano, B. Ruggiero, and E. Sarnelli
Istituto di Cibernetica del Consiglio Nazionale delle Ricerche, Via Toiano 6, I-80072 Arco Felice, Italy
(Received 8 June 1990)

The static configurations of a long Josephson junction in the presence of an external magnetic field are investigated. The theoretical analysis is based on the phase-space configurations of the perturbed sine-Gordon equation in the time-independent case. The proposed method allows one to compute in a very simple way the dependence of the Josephson current on the magnetic field for arbitrary junction lengths.

INTRODUCTION

The investigation of the static and dynamic properties of long Josephson junctions, i.e., junctions with dimensions larger than the Josephson penetration depth[1] λ_j, is of great interest in both basic and applied physics. Long Josephson junctions can support, under particular conditions, the propagation of nonlinear waves, fluxons, providing an ideal testing ground for the models of soliton propagation in nonlinear media.[2] Moreover, since each fluxon is associated with a magnetic flux quantum, their periodic motion in long junctions generates an electromagnetic field in the microwave-frequency region. Devices based on this effect have been proposed to build millimeter and submillimeter wave generations for applications in radioastronomy and space communications.[3]

The progress in the understanding of long-Josephson-junction dynamics has slowed down because, in general, analytical solutions of the nonlinear wave equation describing the junction dynamics do not exist. Thus, only perturbative[4] and numerical[5] methods have been used.

In the static case, i.e., when no time dependence of the fields in the junction is considered, the wave equation may be simplified considerably. This allows the use of analytical methods,[6,7] which provide important information on possible junction configurations and, consequently, on possible dynamical states.

In the case of in-line geometry junctions, Owen and Scalapino[7] have developed a numerical method that provides the dependence of the Josephson critical current on the external magnetic field for arbitrary junction lengths.

In this paper, using a phase-space analysis, the possible static configurations relative to a long Josephson tunnel junction with uniform bias current are investigated, and their dependence on the external bias current and the applied magnetic field is obtained.

In the first section the theoretical approach for the phase-space analysis is shown, and some analytical results valid for very long junctions are derived.

The second section deals with finite-length junctions. In this case a fully analytical treatment is not possible, and a very fast and simple numerical method, based on the phase-space analysis, has been developed providing the full magnetic-field dependence of the Josephson critical current for any junction length.

Finally, further improvements to the proposed method are discussed.

PHASE-SPACE ANALYSIS

The electrodynamics of a long, overlap geometry Josephson junction are described by a perturbed sine-Gordon equation,[8] which, in normalized form, is

$$\phi_{xx}-\phi_{tt}-\sin\phi=\alpha\phi_t-\beta\phi_{xxt}-\gamma\ , \tag{1}$$

where ϕ is the phase difference between the two superconductors, α is the normalized junction conductance, β is the normalized superconductor surface conductance, and γ is the dc bias current, here assumed spatially uniform, normalized to the maximum Josephson current. As usual,[1] x is normalized to the Josephson penetration depth λ_j, and t is normalized to the inverse of the angular plasma frequency ω_j. Subscripts in Eq. (1) denote partial derivatives. The phase ϕ is related to the relevant electromagnetic quantities in the junction, since ϕ_t is proportional to the voltage across the barrier and $\phi_x+\beta\phi_{xt}$ to the surface current (ϕ_x being the normalized Cooper-pair current and $\beta\phi_{xt}$ the normalized quasiparticle current).

The appropriate boundary conditions for this geometry are

$$\phi_x(0,t)+\beta\phi_{xt}(0,t)=\phi_x(L,t)+\beta\phi_{xt}(L,t)=\eta\ , \tag{2}$$

where L is the normalized junction length, and η is the normalized external dc magnetic field.

The time-independent configurations of the junction are solutions of Eqs. (1) and (2), where the time derivatives are neglected:

$$\phi_{xx}-\sin\phi=-\gamma\ , \tag{3a}$$

$$\phi_x(0)=\phi_x(L)=\eta\ . \tag{3b}$$

If in Eqs. (3) t replaces x and a new phase $\psi=\phi-\pi$ is defined, the equation for a simple pendulum with a constant applied torque γ is obtained. In this framework the boundary conditions (3b) will become constraints on the initial and final pendulum angular velocity. Thus, follow-

ing this analogy, all the possible static configurations of the phase in a long junction correspond to dynamical configurations of a simple pendulum, subject to a constant torque and to boundary conditions on its velocity.

In the absence of external magnetic field ($\eta=0$), a solution of Eq. (3a) is, for $-1<\gamma<1$, simply $\phi=\arcsin\gamma$, and corresponds to the stable equilibrium position of the pendulum.

Equation (3a) can be integrated, yielding

$$\phi_x(K,\gamma,\phi)=\pm[2(K-\gamma\phi-\cos\phi)]^{1/2}\ , \tag{4}$$

where K is an integration constant.

Equation (4) defines the phase space of Eq. (3a), as is shown in Fig. 1 for $\gamma=0.3$ and different values of K. As it is clear from Eq. (4), the phase plane is symmetric with respect to the $\phi_x=0$ axis and replicates itself under a phase shift of $2\pi n$ (with n integer), provided that the integration constant K is redefined as $K'=K-2n\pi\gamma$. For $\gamma<1$, Eq. (3a) admits two infinite sequences of fixed points:

$$A_n\equiv(\arcsin\gamma\pm2n\pi,0)$$

and

$$B_n\equiv(\pi-\arcsin\gamma\pm2n\pi,0)\ .$$

The points B_n and A_n correspond to stable and unstable static pendulum configurations, respectively.

In the following, the case $n=0$ will be considered, since the extension to the $n\neq0$ case can be obtained by a simple phase redefinition.

In Fig. 1, two families of closed and open curves are shown, the closed curves surrounding the fixed point B_0. The two sets of curves are separated by a curve (the separatrix) containing the fixed point A_0.

The particular case of a semi-infinite junction will be considered first. In this case the external magnetic field is assumed to influence only the $x=0$ edge of the junction, while, on the $x\to\infty$ side, there is no external field ($\eta=0$), and the phase ϕ relaxes to the equilibrium value: $\phi=\arcsin\gamma$. Hence, the boundary conditions (3b) become

$$\phi_x|_{x=0}=\eta,\quad \phi_x|_{x\to\infty}=0,\quad \phi|_{x\to\infty}=\arcsin\gamma\pm2n\pi\ . \tag{5}$$

The boundary conditions (5) imply that all the solution curves must end in a fixed point A_n and, therefore, lie on a separatrix. In Fig. 1, for instance, five branches can be identified, all satisfying the boundary conditions (5): CA_0, EA_0, DEA_0, DA_0, and EDA_0. Once the phase is known, the x dependence of the phase can be easily obtained by integrating ϕ_x^{-1} along the corresponding branch in the phase plane, e.g., the branch starting in the point C in Fig. 1:

$$x=\int_{\phi_c}^{\phi(x)}\phi_x^{-1}\,d\phi\ . \tag{6}$$

Inserting the boundary condition (5) into Eq. (4), an expression for the integration constant K is obtained, corresponding to the separatrix:

$$K^*=(1-\gamma^2)^{1/2}+\gamma\arcsin\gamma\ . \tag{7}$$

Substituting K^* into Eq. (4) with Eq. (7), the analytical expression for the separatrix, shown as a solid curve in Fig. 1, is obtained:

$$\phi_x=\pm\{2[(1-\gamma^2)^{1/2}+\gamma\arcsin\gamma-\cos\phi-\gamma\phi]\}^{1/2}\ . \tag{8}$$

Since the separatrix tends to the point A_0 with linear slope, the integral in Eq. (6) computed along a branch containing the point A_0 tends to infinity. Hence, the corresponding solution belongs to an infinite length junction.

The arrows in Fig. 1 denote the direction along which the x variable increases. Therefore, the first three branches, CA_0, EA_0, and DEA_0, represent solutions for a semi-infinite junction, having the point A_0 at $x=+\infty$, while the latter two branches, DA_0 and EA_0D, represent solutions having the point A_0 at $x=-\infty$.

In Fig. 2 several separatrices, corresponding to different values of the bias current γ, are shown. It is worth noting that, for $\gamma>0$, the separatrices are not

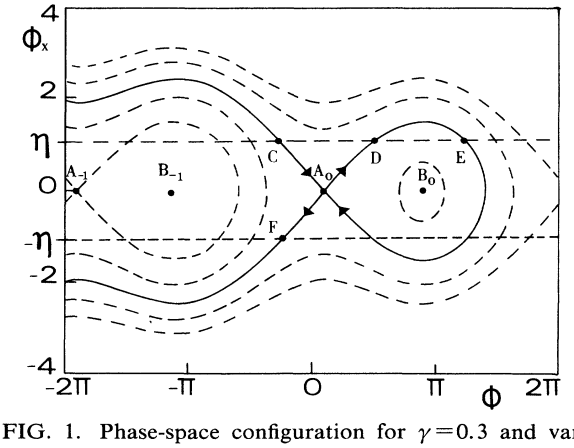

FIG. 1. Phase-space configuration for $\gamma=0.3$ and various values of the integration constant K. The continuous line is the separatrix and contains the stable fixed point $A_0\equiv(\arcsin\gamma,0)$. $B_0\equiv(\pi-\arcsin\gamma,0)$ is the unstable fixed point and η is the normalized dc external magnetic field.

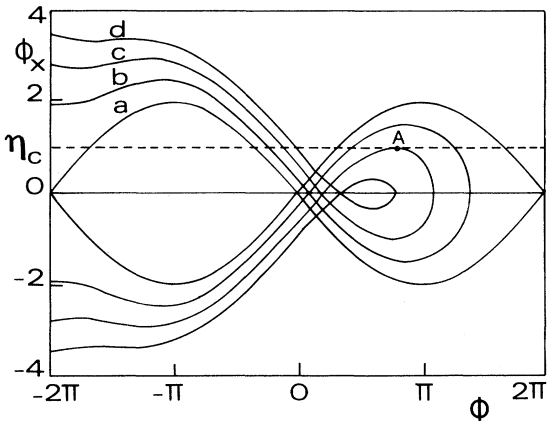

FIG. 2. Separatrices for different values of the normalized bias current γ: (a) $\gamma=0$;, (b) $\gamma=0.3$, (c) $\gamma=0.6$, and (d) $\gamma=0.9$. η_c is the critical magnetic field for $\gamma=0.3$. The abscissa of the point A gives the value of the phase at the point $x=0$.

bounded in ϕ_x. In the case of a semi-infinite junction lying on the negative x axis, and in the presence of a magnetic field η, the phase configuration will be described by the branches DA_0 and EA_0D of Fig. 1 for $\eta>0$ and by the branch FA_0 for $\eta<0$.

For a fixed positive magnetic field η and increasing the bias current γ, the points D and E in Fig. 1 get closer until they coincide (point A in Fig. 2) at a particular current value γ^* ($\gamma^*=0.6$ for the case shown in Fig. 2). For $\gamma>\gamma^*$, there are no more branches satisfying the given boundary conditions, indicating that static phase configurations are not possible.

In this case the combined action of the bias current γ and of the magnetic field η is such that flux quanta enter the junction from the $x=0$ edge and are driven toward the other edge ($x=+\infty$) by the bias current, leading to a situation similar to the flux flow configuration often observed in long junctions.[3]

The value of the phase at the point A is readily computed from Eq. (8), obtaining $\phi_A=\phi_{B_0}=\pi-\arcsin\gamma^*$. Inserting ϕ_A for ϕ and η for ϕ_x into Eq. (8), the η versus γ^* relation, describing the boundary of existence of static solutions, is obtained as

$$\eta(\gamma^*)=2[(1-\gamma^{*2})^{1/2}+\gamma^*\arcsin\gamma^*-\gamma^*\pi/2]^{1/2} . \quad (9)$$

For $\eta<0$ and for any value of γ ($0<\gamma<1$), there is always an intersection between the separatrix and the $\phi_x=\eta$ line (e.g., point F in Fig. 1) thus giving $\gamma^*=1$.

Figure 3 shows the magnetic-field pattern $\gamma^*(\eta)$ [Eq. (9)], for a semi-infinite junction. The "plateau" effect in Fig. 3 is a peculiarity of a semi-infinite junction; indeed, for $\eta<0$, there is a balance between the magnetic field, which tends to inject antifluxons (flux quanta with opposite sign) into the junction, and the bias current, which tends to drive them out. An equilibrium situation is reached when a number (which depends on γ) of antifluxons is trapped in the junction. Hence, there will always be a static configuration for $\gamma<1$.

From an experimental point of view, a semi-infinite junction can be simulated by a long but finite overlap junction with a magnetic field localized at one edge only. This situation well approximates the boundary conditions (5). A similar phenomenon has been reported in an experiment by Nagatsuma *et al.*[9] In their case, there was the same magnetic field on both junction ends but no current bias on one end. This implies that, on the unbiased end, a flux quantum penetrates the junction only when the external field reaches the critical value $\eta_c(0)=2$, thus generating a plateau in the magnetic-field diffraction pattern for $0<\eta<2$.

It is worth noting that the pattern in Fig. 3 (continuous line) for negative fields is different from the one obtained by Kupriyanov *et al.*[10] (dashed curve in Fig. 3). In fact, in the latter case, the authors considered a very long but finite junction. The appropriate boundary conditions are, in this case, given by Eq. (3b) rather than Eq. (5). As a consequence, the magnetic-field pattern is given by Eq. (9) for both positive and negative fields.

FINITE-LENGTH JUNCTIONS

In the finite-length case, a complete analytical treatment is not possible, and numerical methods are needed. The phase configuration inside the junction is described by Eq. (4), provided that the boundary conditions (3b) are satisfied. Such solutions are shown in Fig. 4 as branches ending with the same ϕ_x value (e.g., curve EB).

The length L of the junction is given implicitly by the integral

$$L=\int_{\phi(0)}^{\phi(L)}\phi_x^{-1}\,d\phi . \quad (10)$$

Here, $\phi(0)$ and $\phi(L)$ are the phases at the branch end points, and the integral is computed along the selected branch. From Eq. (10) it is clear that a finite-length junction cannot be described by curves containing the fixed

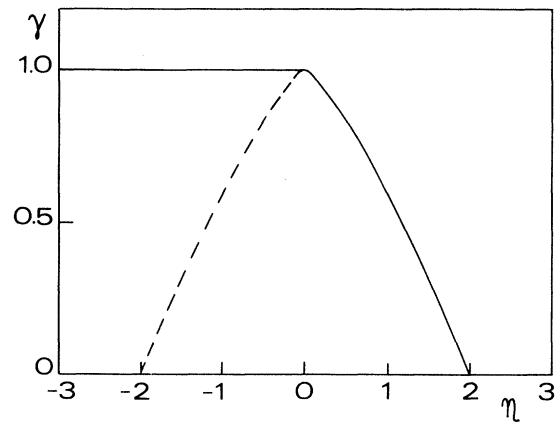

FIG. 3. Theoretical magnetic-field dependence of the Josephson critical current for a semi-infinite junction lying along the negative x axis (continuous line) and for a very long but finite (dashed line) overlap junction. A plateau is obtained in the semi-infinite case.

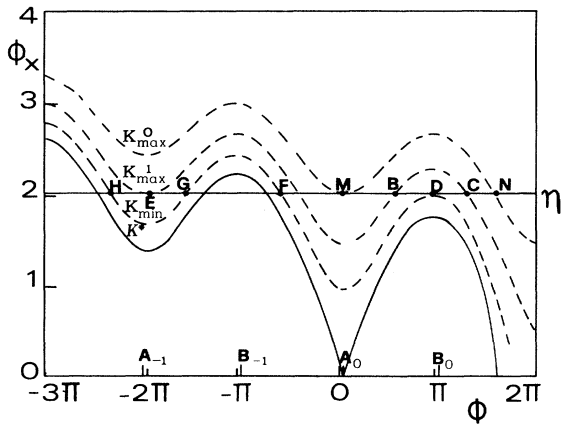

FIG. 4. Phase-space diagrams for $\gamma=0.3$. $K_{\min}$, $K^0_{\max}$, $K^1_{\max}$, and K^* identifying, respectively, the curves tangent to $\phi_x=\eta$ at the first maximum to the right of A_0 (point D), at the point M, at the first minimum on the left of the A_0 (point E), and the separatrix.

point A_0, otherwise the computed length would be infinite.

In the absence of an external magnetic field ($\eta=0$), the boundary conditions (3b) require that the only possible solutions correspond to the fixed ponts A_0, B_0, and to the branches surrounding the unstable point B_0, starting and ending with $\phi_x=0$ (see Fig. 1). However, only point A_0 represents the stable solution of the junction.

For $\eta\neq 0$, among all the possible branches only those spanning over the stable pendulum equilibrium point A_0 (e.g., curve EB in Fig. 4) are considered neglecting those spanning the unstable point B_0 (e.g., curves EC and BC in Fig. 4). This choice is somewhat arbitrary since, within the present model, the stability of each possible solution cannot be determined, and the criterion that has been adopted is to consider stable the solution that is closer to the stable equilibrium solution in absence of external magnetic field η (point A_0).

For a given value of γ, the solutions related to m magnetic flux quanta (fluxons) trapped in the junction have to satisfy the condition

$$2m\pi \leq |\phi(L)-\phi(0)| \leq 2(m+1)\pi \ . \tag{11}$$

The case with less than one fluxon trapped in the junction ($m=0$) will now be considered. The first thing to note is that by increasing the value of K in Eq. (4), the corresponding curves in Fig. 4 move toward higher positions. Therefore, for a given value of η, there will be a minimum value of K,

$$K_{\min}=\frac{\eta^2}{2}+\gamma\pi-K^* \ , \tag{12}$$

for which there is an intersection on the right of the point A_0 (point D in Fig. 4) between the line $\phi_x=\eta$ and the curve described by Eq. (4).

Similarly, there will be a maximum value of K

$$K^0_{\max}=\frac{\eta^2}{2}+K^* \tag{13}$$

for which there is an analogous intersection on the left-hand side of the point A_0 (point M in Fig. 4).

All the possible solutions (in the $m=0$ case) are obtainable for $K_{\min}\leq K\leq K^0_{\max}$. Moreover, from Eq. (10), it is evident that the curve with $K=K_{\min}$ corresponds to the minimum allowed length value

$$L_{\max}(\gamma,\eta)=\int_{\phi_F}^{\phi_D}\phi_x^{-1}(K_{\min},\gamma,\phi)d\phi \ , \tag{14}$$

and that the curve with $K=K_{\max}$ corresponds to the minimum one,

$$L^0_{\min}(\gamma,\eta)=\int_{\phi_M}^{\phi_M}\phi_x^{-1}(K^0_{\max},\gamma,\phi)d\phi=0 \ . \tag{15}$$

ϕ_F is determined by solving equation

$$\phi_x(K_{\min},\gamma,\phi)=\eta \ , \tag{16}$$

using a root-finder algorithm based on the bisection method. ϕ_D and ϕ_M are easily found as $\phi_D=\phi_{B_0}=\pi-\arcsin\gamma$ and $\phi_M=\phi_{A_0}=\arcsin\gamma$.

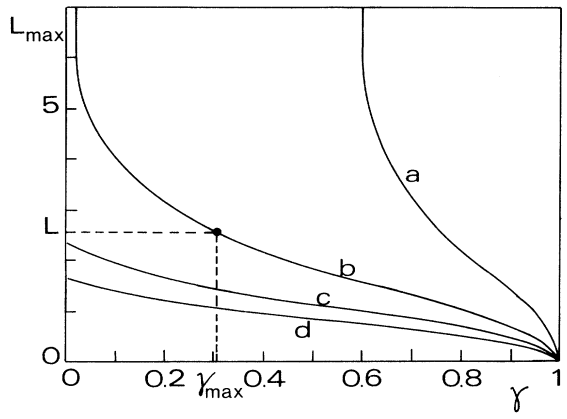

FIG. 5. Maximum junction length ($L_{\max}$) vs bias current γ for four values of the external magnetic field in the $m=0$ case: (a) $\eta=1$, (b) $\eta=2$, (c) $\eta=3$, and (d) $\eta=4$. $\gamma_{\max}$ is the value of γ for which $L_{\max}=L$.

In Fig. 5, the dependence of $L_{\max}$ on γ [Eq. (14)] is shown for various values of η. In order to obtain the dependence of the critical current on the external magnetic field for zero fluxons trapped and for a particular junction length L, the equation $L_{\max}(\gamma_{\max},\eta)=L$ (see Fig. 5) is solved numerically for γ using the same algorithm quoted before. $\gamma_{\max}$ is the maximum current value compatible with the existence of a static solution, and, therefore, the dependence of $\gamma_{\max}$ on η represents a lobe of magnetic-field diffraction pattern for the junction of length L.

COMPLETE MAGNETIC PATTERN

Similarly to the $m=0$ case, there is a maximum value for K for $m\neq 0$, i.e., when m fluxons are trapped into the junction

$$K^m_{\max}=\frac{\eta^2}{2}+K^*-2m\gamma\pi \ , \tag{17}$$

for which there is an intersection on the left-hand side of

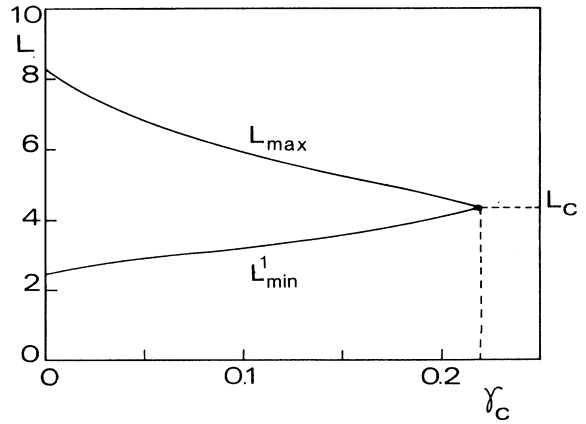

FIG. 6. $L_{\max}$ and $L^1_{\min}$ of the bias current γ for $\eta=2.2$ and $m=1$. The region between the two curves identifies the locus of the allowed junction lengths.

the point A_{-m}, between the line $\phi_x=\eta$ and the curve described by Eq. (4). Hence, all the possible solutions lie on branches with $K_{\min}<K<K^m_{\max}$.

An expression for $L^m_{\min}$ and $L_{\max}$ can be written (referring to Fig. 4 for $m=1$) as

$$L_{\max}(\gamma,\eta)=\int_{\phi_G}^{\phi_D}\phi_x^{-1}(K_{\min},\gamma,\phi)d\phi \tag{18}$$

and

$$L^1_{\min}(\gamma,\eta)=\int_{\phi_E}^{\phi_B}\phi_x^{-1}(K^1_{\max},\gamma,\phi)d\phi\ . \tag{19}$$

ϕ_G and ϕ_B are determined by numerically solving the equations $\phi_x(K_{\min},\gamma,\phi)=\eta$ and $\phi_x(K^1_{\max},\gamma,\phi)=\eta$, respectively, while $\phi_E=\phi_{A_{-1}}=\arcsin\gamma-2\pi$. It is important to note that, unlike the $m=0$ case, $L^m_{\min}$ is now, in general, different from zero.

In Fig. 6, the dependence of $L_{\max}$ and $L_{\min}$ on γ for $\eta=2.2$ and $m=1$ is shown. The allowed junction lengths are in the dashed region of the figure.

Numerically solving the equations $L_{\max}(\gamma_{\max},\eta)=L$ and $L^m_{\min}(\gamma_{\max},\eta)=L$ is now possible to compute $\gamma_{\max}(\eta)$ for any lobe m, obtaining the complete dependence of the Josephson critical current on the magnetic field.

In Fig. 7, the magnetic patterns for three junction lengths ($L=2,4,7$) are shown. These lengths are representative of the three different regimes typically observed, i.e., small, intermediate, and long junction. It is interesting to note that the pattern in the finite length case is very close to the asymptotic limit already for $L=7$. On the other hand, the pattern for $L=2$ closely follows the Fraunhofer-type behavior ($L\to 0$), showing that the intermediate length region, where the junction response deviates significantly from the known limit cases, is confined to $2<L<7$.

A critical situation occurs when $K_{\min}=K^m_{\max}$. This condition implies the existence of a critical value γ_c (see Fig. 6):

$$(1-\gamma_c^2)^{1/2}+\gamma_c\arcsin\gamma_c=\frac{2m+1}{2}\pi\gamma_c\ . \tag{20}$$

The solutions of this equation correspond to the maximum current values for each lobe m in the magnetic diffraction pattern of a very small junction. This result is valid also for the junction length considered and is due to the assumption of an uniform bias current.

It is also worthwhile to note that γ_c corresponds to the crossover length L_c from the $L^m_{\min}(\gamma)$ and the $L_{\max}(\gamma)$ curve (Fig. 6).

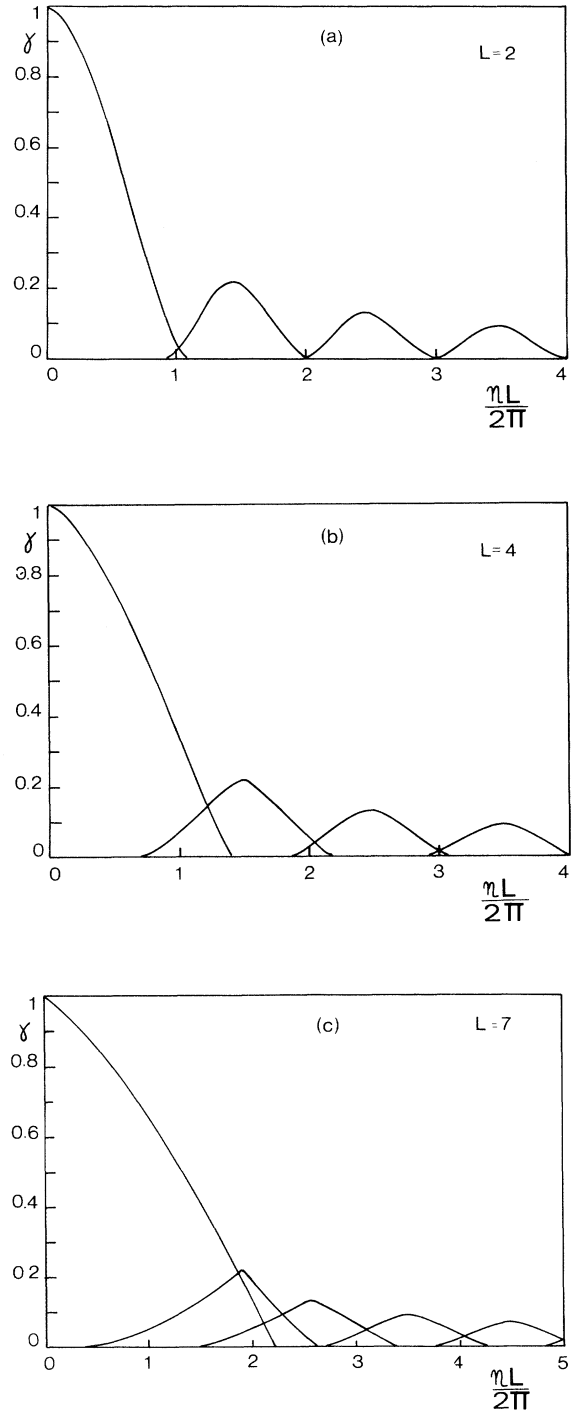

FIG. 7. Theoretical dependences of the Josephson critical current on the external magnetic field for different junction lengths: (a) $L=2$, (b) $L=4$, and (c) $L=7$.

CONCLUSIONS

The method developed enables one to compute the magnetic field dependence of the critical current in Josephson junctions of any length with uniform bias current for an overlap geometry. This method is based on a general approach, which, however, has some limitations. Indeed, as it is evident in Fig. 4, for $m=1$, there are several possible choices for a branch satisfying the constraints on the phase variation Eq. (11), (e.g., the branches GD and HD for $K=K_{\min}$ and EB and EC for $K=K_{\max}$). Only the branches spanning over stable equilibrium points A_m have been considered, assuming such solutions to be more stable than the others. A detailed stability analysis of all the possible solutions should, how-

ever, be performed in order to determine the configurations that can be experimentally observed.

This approach can be extended to treat junctions of in-line geometry, for which analytical results are already available,[7] and to junctions with a mixed in-line and overlap bias configuration.[11] Work is in progress in this direction both on the analytical and the experimental side.

ACKNOWLEDGMENTS

The authors are grateful to C. Salvia for technical support. This work was partially supported by the European Economic Community through Contract No. ST-2-0267-J-C(A), and by the Consiglio Nazionale delle Richerche through the Progetto Finalizzato "Superconductive and Cryogenic Technologies."

[1]A. Barone and G. Paternò, *Physics and Applications of the Josephson Effect* (Wiley, New York, 1982).

[2]P. L. Christiansen and O. H. Olsen, Wave Motion **2**, 185 (1980).

[3]T. Nagatsuma, K. Enpuku, F. Irie, and K. Yoshida, J. Appl. Phys. **54(6)**, 3302 (1983).

[4]D. W. Mc Laughlin and A. C. Scott, Phys. Rev. A **18**, 1652 (1978).

[5]O. H. Olsen, N. F. Pedersen, M. R. Samuelsen, H. Svensmark, and D. Welner, Phys. Rev. B **33**, N1, 168 (1986).

[6]S. Pace, M. Cirillo, and S. Pagano, Jpn. J. Appl. Phys. **26**, 1571 (1987).

[7]C. S. Owen and D. J. Scalapino, Phys. Rev. **164**, 538 (1967).

[8]R. D. Parmentier, in *Solitons in Action,* edited by K. Lonngren and A. Scott (Academic, New York, 1978), pp. 173–199.

[9]T. Nakatsuma, E. Enpuku, K. Sucoka, K. Yoshida, and F. Irie, J. Appl. Phys. **58**, 441 (1985).

[10]M. Y. Kupriyanov, K. K. Likharev, and V. K. Semenov, Fiz. Nizk. Temp. **2**, 1252 (1976) [Sov. J. Low Temp. Phys. **2**, 610 (1976)].

[11]M. R. Samuelsen and S. A. Vasenko, J. Appl. Phys. **57**, 110 (1985).